Journal of Applied Polymer Science

Solvent Diffusion in Silica/Poly[styrene-*co*-(acrylic acid)] Core-Shell Microspheres by Pulsed Field Gradient NMR Techniques

Binbo Jiang,[1] Yong Yang,[1] Lijun Du,[2] Carlos Mattea,[3] Jingdai Wang,[1] Siegfried Stapf,[3] Yongrong Yang[1]

[1]Department of Chemical and Biochemical Engineering, State Key Laboratory of Chemical Engineering, Zhejiang University, Hangzhou 310027, Zhejiang, People's Republic of China

[2]Shanghai 3F New Material Co., Ltd., Shanghai 200241, China

[3]Fachgebiet Technische Physik II/Polymerphysik, Institut für Physik, TU Ilmenau, 98684 Ilmenau, Postfach 10 05 65, Germany

Correspondence to: W. Jingdai (E-mail: wangjd@zju.edu.cnl)

ABSTRACT: Polymer-coated SiO_2 particles are prepared by precipitation of poly[styrene-*co*-(acrylic acid)] on SiO_2 microspheres through an improved phase inversion method. The diffusion resistance of the polymer membrane was considered to be the critical reason for producing tailor-made polyethylene by catalysts supported on these polymer-coated particles. This paper employs pulsed field gradient NMR (PFG-NMR) to distinguish diffusion of *n*-hexane in different regimes, i.e., in the space between each particle, the pores in SiO_2 and the polymer shell, by their respective diffusion coefficients. By varying the observation time, the time scale of the molecular exchange is discussed. A three-region ansatz was used to interpret the exchange and diffusion in polymer-coated SiO_2 system, and was compared with results acquired with noncoated particles. At long diffusion times, the mean-squared displacement, and thus the averaged self-diffusion coefficient, of hexane in the system of polymer-coated SiO_2 particles is significantly reduced. The PSA membrane is identified as an efficient barrier against molecular exchange between the pores in SiO_2 and the intraparticle space. Consistently, the relaxation measurements indicated that the mobility of *n*-hexane molecules, especially the rotation of *n*-hexane, was limited by the PSA membrane. © 2013 Wiley Periodicals, Inc. J. Appl. Polym. Sci. **2014**, *131*, 40161.

KEYWORDS: composites; properties and characterization; adsorption

Received 9 September 2013; accepted 5 November 2013

DOI: 10.1002/app.40161

INTRODUCTION

Diffusion through a rate-controlling membrane leads to multiple applications of polymer-coated particles.[1] Most polymer-coated particles are designed as capsules for diffusive release of active materials[2,3] while also a few were applied in the catalysis field.[4–6] Previously, single polymer-supported[7,8] or organic-supported catalysts[9,10] were successfully synthesized and applied in the conventional polymerization process. In the recent development of heterogeneous catalysts, tailor-designed catalysts are needed for pursuing higher-performance product.[10] And polymer-coated particles used as the support of polyolefin catalysts[11,12] are one approach to realized tailor-designed catalysts.

Guo et al.[13] and Kaur et al.[14] made an effort to immobilize metallocene and Ziegler-Natta catalysts on inorganic/polymer composite supports and obtained some exciting results. However, a thorough discussion of the role of the polymer in the support was not given. Our group has synthesized silica/poly [styrene-*co*-(acrylic acid)] (SiO_2/PSA) microspheres by phase inversion principles and has successfully applied them as supports of polyolefin catalysts.[12,15] These functional supports promoted the performance of the resulting catalysts. Compared with the polyethylene produced by normal silica-supported catalysts, polyethylene with a broad molecular weight distribution was obtained by the catalyst supported on these polymer-coated particles. The tunable properties of the polymer membrane, which can be introduced with different thickness, were critical for interpretation of the ethylene polymerization results. We supposed that the PSA membrane possesses different mass transport capabilities to the reactants. This conclusion was indirectly deduced based on the results of ethylene polymerization. We therefore intend to obtain direct data of liquid diffusion in the polymer-coated particles, a topic that has, due to the complexity of the system, not been treated in detail so far. Accurate and reliable determination of diffusion coefficients of small molecules in polymer-coated particles is valuable for an improved understanding of the ethylene polymerization by heterogeneous catalyst on the polymer-coated support.

Conventional methods for measuring the diffusion coefficients, such as bulk equilibration,[16] gravimetric vapor sorption/desorption[17] and gas chromatography[18] measurements are time consuming or require elaborate procedures. The critical disadvantage of these methods is that they are not able to obtain more than one averaged diffusion coefficient. Pulsed field gradient NMR is a powerful method for the measurement of liquid diffusion in porous media[19,20] and has been applied in the characterizations of the core-shell particles.[21,22] Analysis of echo decays obtained for different diffusion times can give information about the time scale of exchange and diffusion in different sites. Based on the principle of diffusion contrast, molecular exchange between different sites has been studied in a number of different colloidal systems. Choudhury and Schonhoff[21] has investigated the permeability of phenol and poly(ethylene oxide) in hollow capsules dispersions by PFG-NMR, respectively. Wassenius et al.[23] used NMR to study the diffusion of oil inside core-shell latex particles. Water diffusion within biological compartments was reviewed by Donahue et al.[24] All studies have been carried out on hollow particles.

Based on our previous work, we focus on investigating the influence of the polymer shell of core-shell particles on the liquid diffusion behavior. Both SiO_2 and polymer-coated SiO_2 were taken into account. The synthesis of polymer-coated SiO_2 was based on the improved phase inversion method reported in Ref. 15. The particle surface morphology was observed by scanning electron microscopy (SEM). The quantitative results of pore size distribution, pore volume, specific surface area, and average pore diameter were obtained from nitrogen adsorption (BET) measurements. The measurements of the diffusion capabilities and relaxation in SiO_2 and polymer-coated SiO_2 are performed by PFG-NMR using *n*-hexane as a probe molecule.

MATERIAL AND METHODS

Sample Preparation

The silica sample used is commercially available SiO_2 spheres (Grade XPO2485 from W. R. Grace & Co.). The silica spheres were dried at 600°C for 4 h in the presence of nitrogen flow before use. Core-shell particles were synthesized by coating a defined amount of poly[styrene-*co*-(acrylic acid)] on SiO_2 based on a procedure proposed by Du et al.[17] All manipulations were either in a glove box or under inert nitrogen atmosphere using standard Schlenk techniques.[25]

Scanning Electron Microscopy (SEM)

The surface morphology of SiO_2 and polymer-coated SiO_2 particles was subsequently investigated by SEM (Hitachi S-4700 field-emission scanning electron microscope), operated 15 kV. Samples observed with Hitachi SEM required coating with a conductive layer. This was performed by sputtering a few nanometers thick layer of gold on the sample under vacuum.

Laser Particle Size Analysis

Volume particle size distribution of the particles was determined by a laser scattering particle analyzer (Malvern Mastersizer 2000). *n*-Heptane was used to disperse the particles. Particle size distribution is characterized by the mass median diameter ($d_{0.5}$), i.e., the size in microns at which 50% of the sample is smaller and 50% is larger, and the volume mean diameter ($D_{4,3}$). Values presented are the average of at least three determinations.

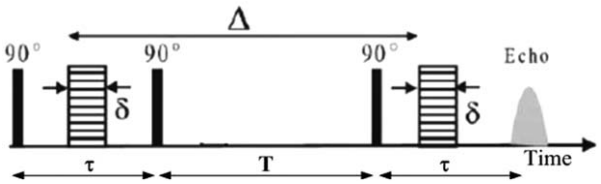

Figure 1. The PFG stimulated echo sequence.

Nitrogen Adsorption/Desorption Measurements

The nitrogen adsorption/desorption measurements were performed at 77 K using a Micromeritics ASAP 200 instrument. The values of the specific surface area were estimated by nitrogen adsorption data in the relative pressure range from 0.05 p/p_0 to 0.30 p/p_0 using the BET equation. The mesopore volume V_p, was determined by means of the BJH method.

NMR Experiments

Liquid *n*-hexane was selected as a probe molecule for NMR diffusion measurements. Before the experiments, 0.30 g packed SiO_2 or polymer-coated SiO_2 particles were saturated with 1.5 mL *n*-hexane in the NMR sample tube of 4 mm inner diameter for at least 72 h.

The ^{1}H longitudinal (T_1) NMR relaxation and diffusion experiments were performed at 7 T on a Bruker Avance III NMR spectrometer, working at a proton resonance frequency of 300 MHz. Uniaxial field gradient coils (DIFF 30) providing a maximum gradient strength of 1200 G/cm were attached for the purpose of diffusion experiments. All measurements were carried out at room temperature (20°C). The gradient coils were cooled by a water circulation unit that also served to control the sample temperature. The ^{1}H longitudinal (T_1) NMR relaxation times were determined employing an inversion recovery pulse sequence with a variable delay time τ between radiofrequency pulses [π-τ-π/2-acquisition]; typically, values of τ between 2 and 15,000 ms were used, and 16 signal accumulations were acquired for each τ value. The self-diffusion coefficients of bulk *n*-hexane and *n*-hexane molecules in SiO_2 or PSA-coated SiO_2 were measured using the pulsed gradient stimulated echo (PGSTE) sequence shown in Figure 1. A pair of magnetic field gradient pulses with duration δ was employed. For each measurement on diffusion of *n*-hexane, the strength of the gradient pulses g with the duration δ of 1.0 ms was varied in 16 steps to the defined maximum value. The diffusion time (Δ) was varied from 5 ms to 500 ms and 32 signals were accumulated for each step.

THEORY

Diffusion in Homogeneous Systems

For a single resonance in an uncoupled spin system, the decay of the signal intensity of the stimulated echo can be described by eq. (1):[26]

$$I(k)=I(0)\exp(-kD)$$
$$k=(\gamma g\delta)^2(\Delta-\frac{\delta}{3}) \quad (1)$$

where I(k) and $I(0)$ are the stimulated echo intensities in the gradient field and in the absence of gradients, respectively. D is the self-diffusion coefficient, γ is the gyromagnetic ratio of the nucleus, g is the gradient strength, δ is the gradient pulse duration, and Δ is the separation between the PFGs, henceforth being approximated as the "diffusion time."

The diffusion coefficient is related to the root mean square (rms) displacement. In a PFG NMR experiment, the displacement along the axis of the field gradient is the only measured subject.[27] The relationship is described by the Einstein- Smoluchowski equation:[28]

$$\overline{(\Delta x)^2}=2D\Delta \quad (2)$$

where Δx is the root mean squared (rms) displacement of molecules.

For *n*-hexane in porous media, the rms displacement possibly depends on the diffusion time in a nonlinear fashion, and the diffusivity of the molecules, in general, will be influenced by the pore space. In the present work, Δ is varied from 5 ms to 500 ms. The self-diffusion coefficient of *n*-hexane in bulk at 22°C is 3.96×10^{-9} m^2/s, which corresponds to three-dimensional root mean square displacements of between 11 and 110 μm (replacing the coefficient "2" in eq. (2) by "6"). These are upper limits for actual average displacements and have to be compared with the domain sizes observed in the system. In porous media, these values are reduced due to the tortuosity of the pore space;[29] for instance, since the pore size of SiO_2 and PSA-coated SiO_2 particles is in the nanometer range, self-diffusion even during the shortest experimental interval will lead to an averaging of diffusion paths and to an effective reduction (time-independent) of the intraparticle self-diffusion coefficient. Considering exchange between the different regions of varying diffusivity, there are a number of models for extracting parameters relevant for the description of the pore space itself and the interaction of the diffusing liquid with this pore space.

Exchange and Diffusion in Two-Region Systems

In the general case, the relative timescale of molecular exchange in the two regions has to be considered.[21,24,29] The behavior of the self-diffusion coefficient of a liquid in a porous media, and also of its relaxation time, is indicative of the existence of three diffusion time scales:

1. Fast exchange: If the exchange between the two regions is fast compared with the diffusion time scale, then eq. (1) is simplified to a single exponential decay with a mean decay constant given as,

$$I(k)=\exp[-k(f_AD_A+f_BD_B)] \quad (3)$$

This implies that the observed diffusion coefficient is a weighted average of the respective decay constants in either region. An analogous expression holds for the relaxation times T_1 and T_2.

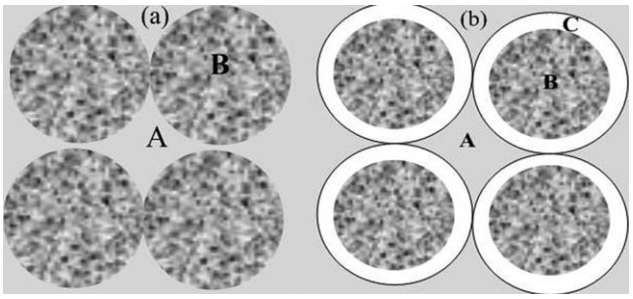

Figure 2. The proposed separated diffusion regions in (a) SiO_2 system and (b) SiO_2/PSA system.

2. Slow exchange: If the molecular exchange between the regions is slow compared with the relevant time scale (i.e. diffusion time), the echo decays in a PFG-NMR experiment are superposition of the corresponding signal decay of molecules in either site. The normalized echo decay can be written as

$$I(k)=(1-P_B)\exp(-kD_A)+P_B\exp(-kD_B) \quad (4)$$

A bi-exponential decay is found in full analogy to the diffusion decay.

3. Intermediate exchange: In between the cases of fast and slow exchange lies "intermediate exchange" where the compartmental diffusion rates and exchange rates have values of the same order of magnitude. This case cannot be described in closed form and requires knowledge of the geometry of the pore space and connectivity; indeed, NMR relaxation and diffusion decays have been suggested as means to extract the pore space morphology.[30]

Diffusion Regions in SiO_2 and SiO_2/PSA Particles

In a system, where a molecule can exist in two separate regions A and B, exchange between the regions affects relaxation and diffusion.[21] In either region the molecules are characterized by a diffusion coefficient $D_{A,B}$ and the relaxation time $T_{1A,B}$. Regarding *n*-hexane in SiO_2 particles [Figure 2(a)], region A is assigned to the confined space between the particles and the mean residence time is τ_A. Region B is the pore space inside the particles, the mean residence time in the pore space is τ_B. The probability of finding the molecules in a given site i is f_i which is given by

$$f_{A,B}=\frac{\tau_{A,B}}{\tau_A+\tau_B} \quad (5)$$

The exchange time τ_{ex} between region A and B can be defined as

$$\frac{1}{\tau_{ex}}=\frac{1}{\tau_A}+\frac{1}{\tau_B} \quad (6)$$

Under certain diffusion-weighting conditions, even simple shapes can lead to intracompartmental apparent diffusion coefficient distributions that are bi- or multimodal. If so, these might be subjected to not only two-region-exchange, but also three-region-exchange or even multiregion-exchange analysis. As shown in Figure 2(b), the core-shell SiO_2/PSA particle can be divided into three separated regions. Region A is the confined space between SiO_2/PSA particles, region B is the pore space of

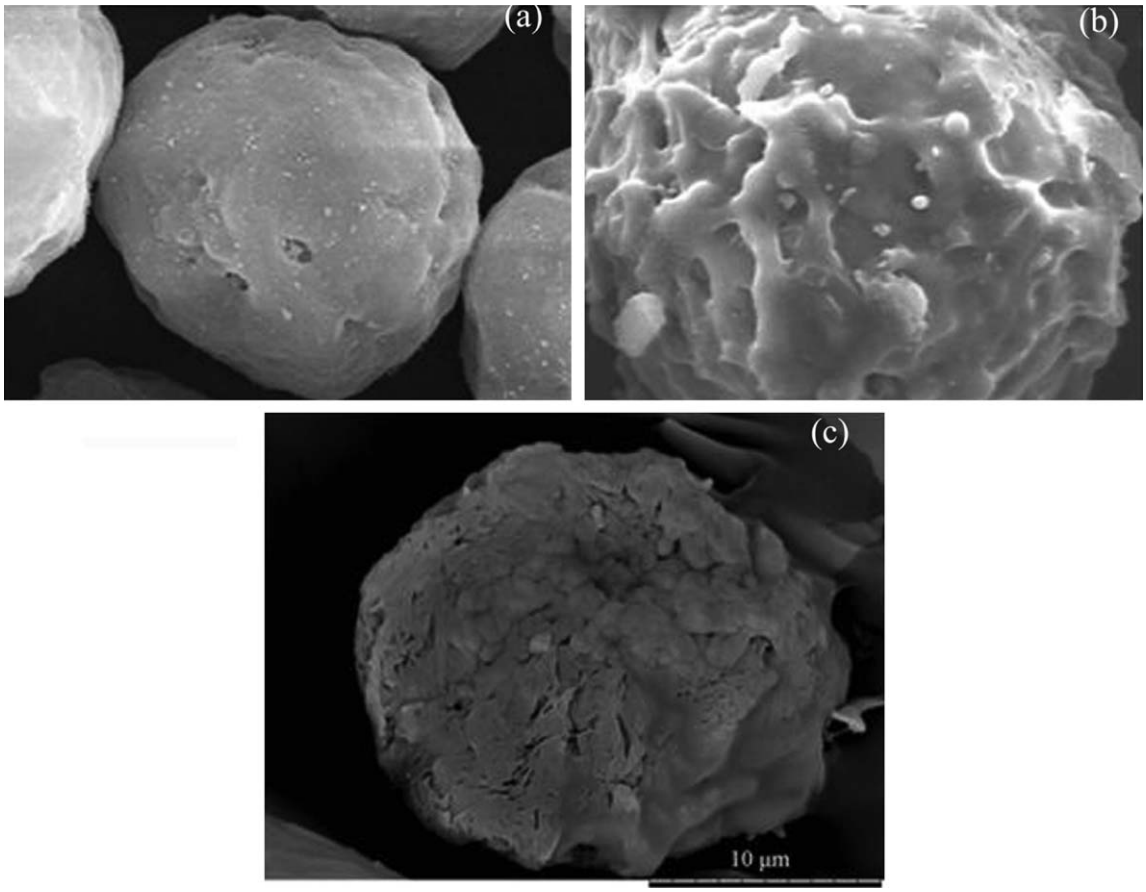

Figure 3. The surface SEM images of silica (a), core-shell particles (b) and the cross-section image of core-shell particles (c).

the core (SiO_2), and region C is the PSA membrane which is also considered porous. Note that swelling of the PSA membrane, which is known to occur in *n*-hexane, can reduce the volume of region A compared with the system of uncoated spheres. The molecular exchange may occur between A and C, and between B and C, each possessing its particular diffusion coefficient. Assuming that the diffusion coefficient in the shell (phase C) is the smallest of the three, it can be understood that the shell acts as a barrier to molecular exchange between the particles and the bulk. The theory of diffusion and exchange in the two-region model needs to be extended for applying it to the particular case of three regions found in this case. We will facilitate discussion by assuming that the intrinsic diffusion coefficients inside the particle (D_B) is the same as in the uncoated system, while the interparticle value, D_A, may be influenced due to partial swelling of the PSA phase, resulting in a smaller available volume. A more detailed discussion of diffusion and exchange in the three-region system will be provided in the following sections.

Relaxation of Liquid in Porous Media

The nuclear magnetic resonance relaxation rates (longitudinal and transverse) are proportional to the spectral density of the autocorrelation function of molecular reorientations; in an approximation that frequently holds for high magnetic fields and small molecules, the value is proportional to the principal correlation time, which often is the average rotation time of the molecule.[31] The average relaxation time under conditions of fast exchange is equal to the inverse of the sum of the weighted relaxation rates for two phases *a*, *b*:

$$\frac{1}{T_1} = \frac{P_a}{T_{1a}} + \frac{P_b}{T_{1b}} \tag{7}$$

Any constraint, such as confinement of a molecule in a porous system or interaction with surfaces, will slow down the reorientational process and thus increase the relaxation rates. For fluids in porous media, the decrease of T_1 and T_2 with decreasing pore size is well-known and is exploited to characterize porous media.[30,32] In this work, measurement of the *n*-hexane longitudinal relaxation time is performed as a probe to identify the respective pore spaces and the exchange processes taking place between them.

RESULTS AND DISCUSSION

Characterization of Core-Shell Structure in the SiO_2/PSA Composite Particles

Our earlier studies, which were concerned with coating PSA on SiO_2, resulted in composite particles with well-defined "core-shell" morphology.[15] In the present work, synthesis of core-shell particles was not the main task. In view of this, high-resolution SEM was used to prove that the SiO_2/PSA particles used in the

Table I. The Particle and Pore Size of SiO_2 and SiO_2/PSA Core-Shell Microspheres

Particles	SiO_2	SiO_2/PSA
Average particle diameter (μm)	21.06	25.24
Average pore size (nm)	21.38	18.68
Porosity (%)	45.57	35.24

diffusion measurements possessed a uniform polymer shell on the surface. This observation confirmed that the surface morphology of the uncoated SiO_2 particles was smooth and featureless [Figure 3(a)]. However, a layer of irregular and rough material is noticeable on the surface of SiO_2/PSA particle [Figure 3(b)]. The core-shell structure is indicated in SiO_2/PSA composite particles. To better identify the PSA membrane, a cross-section SEM photograph was taken. Two separate parts with different structure are shown in Figure 3(c). The outer part, bearing resemblance to the cross-section of a cabbage, is the PSA membrane. The thickness of the PSA membrane is 2 to 3 μm.

The particle size and pore structure parameters are listed in Table I. According to the average diameter (volume-average particle diameter) of SiO_2 and PSA-coated SiO_2, determined by laser particle-size analyzer, one can estimate the average thickness of the PSA membrane to be (25.24–21.06 μm)/2 = 2.09 μm, in agreement with the result of cross-section SEM. The porosity of SiO_2/PSA were much smaller than that of SiO_2. The porosity of SiO_2/PSA is 35.47% while the porosity of SiO_2 is 45.57%. Further, the average pore size of the particle decreased from 21.38 nm to 18.68 nm after SiO_2 was coated by PSA. The lower porosity and smaller average pore size of SiO_2/PSA indicate that the porosity of PSA is low.

Comparison of Spin Lattice Relaxation of *n*-Hexane in Different Systems

Spin-lattice relaxation experiments are performed and evaluated for *n*-hexane in bulk phase and the particles. The obtained signal attenuation curves are given in Figure 4. The spin-lattice relaxation of hexane either in bulk system or in heterogeneous system is single exponential. The measured T_1 for bulk hexane, the silica system and the core-shell particles system are 3.58 s, 2.23 s, and 1.80 s, respectively. The occurrence of a single exponential fitting may be the result of fast, relative to T_1, exchange of *n*-hexane between the intra- and inter-particle spaces. The molecules can diffuse (assuming $D = 1 \times 10^{-9}$ m^2/s, see below) at least 80 μm in 1 s, a range much larger than the particle size. As a result, fast exchange is expected for all T_1 measurements. If we assume the bulk value of 3.58 s to be the correct one for intra-particle hexane, then one can estimate the T_1 inside the pores by weighted averages of the relaxation rates; assuming a packing density of 60%, an actual relaxation time of about 1.4 s is calculated for the T_1 inside the pores based on eq. (7). The relaxation time in the SiO_2/PSA particle decreases further to about 1.0 s; this is in agreement with an individual T_1 inside the PSA membrane of about 0.5 s. In these estimations, the average porosity valued from Table I has been used for estimating a porosity of about 20% inside the PSA coating layer.

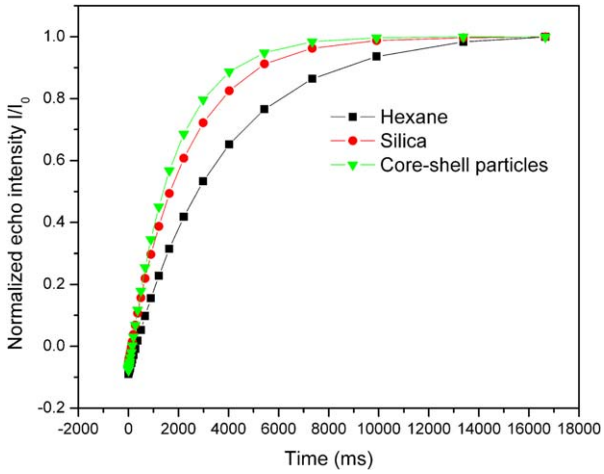

Figure 4. The spin-lattice relaxation curves obtained using inversion-recovery sequence. [Color figure can be viewed in the online issue, which is available at wileyonlinelibrary.com.]

Considering the small thickness of this layer, fast exchange conditions appear justified if rms displacements much exceed the layer thickness; this is ensured for any diffusion coefficient larger than about 10^{-11} m^2/s—it is reasonable to assume that these conditions are fulfilled (see below). It can thus be concluded that the PSA membrane possesses smaller porosity and generates more hindrance to the molecular reorientation; nevertheless, molecular exchange is completed on a timescale of T_1, i.e. on the order of 1 s.

Diffusion of *n*-Hexane in SiO_2 Particles

Diffusion experiments by the PFG NMR stimulated echo sequence were performed for different diffusion times ranging from 5 to 500 ms. In order to cover a comparable range of decays, the gradient strength was varied accordingly for different diffusion times. Attenuation curves of diffusion in SiO_2 are given in Figure 5. All curves exhibit biexponential echo decays,

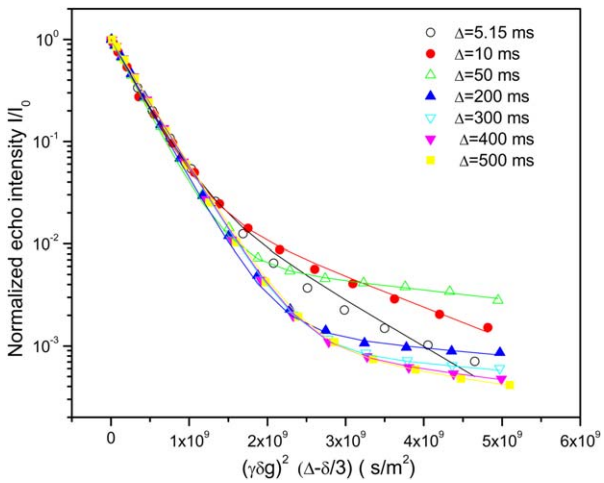

Figure 5. Echo decay curves of the PFG stimulated echo sequence in SiO_2 system. The solid line is the result of biexponential fits to each decay curve. [Color figure can be viewed in the online issue, which is available at wileyonlinelibrary.com.]

Table II. The Calculated Diffusion Coefficients of *n*-Hexane in SiO_2

Diffusion time (ms)	D_A ($\times 10^{-9}$ m^2/s)	rms displacement (μm)	D_B ($\times 10^{-9}$ m^2/s)	rms Displacement (μm)
5.15	3.34	5.86	0.703	3.27
10	3.36	8.20	0.692	3.72
50	3.39	18.41	0.201	4.48
200	3.16	35.55	0.168	8.20
300	2.86	41.42	0.143	9.26
400	2.87	47.92	0.230	13.56
500	2.79	52.82	0.270	16.43

indicating the presence of two localizations of *n*-hexane with different diffusion coefficients.

The apparent diffusion coefficient for either region (D_A and D_B) is given in Table II. The diffusion coefficient of *n*-hexane in bulk phase at 22°C is 3.96×10^{-9} m^2/s. For the diffusion coefficient of *n*-hexane in the space between SiO_2 particles (region A), D_A was smaller and showed hardly any variation with increasing diffusion time. This means that the mobility of *n*-hexane in region A is limited compared with the homogeneous *n*-hexane. However, this limitation is found to be almost constant under the scale of diffusion time here, which indicates pure geometrical restriction as a consequence of the tortuosity of a packed-bead system of typically between 1.5 and 2. The eventual decrease is assigned to averaging effects with the lower mobility inside the porous system (full exchange should render an intermediate value). The other component diffuses more slowly with value D_B and strongly depends on the observation time. This component can be attributed to the fraction of *n*-hexane in the pores inside the particles. We note that the average pore size of SiO_2 is 21.38 nm. Such small size, combined with the intraparticle porosity, leads to restricted diffusion of *n*-hexane. Calculating with the fitted values, the rms displacement is in the order of several μm, far exceeding the pore dimension but still somewhat smaller than the sphere size for the shortest diffusion times. The biexponential behavior points at an incomplete, i.e. slow—compared with Δ—exchange between both regions with an exchange time $\tau_{ex} > \Delta$.

However, as evident from Figure 6, with increasing observation time, D_B first decreases and then increases. It has to be noted that, for diffusion times of 50 ms and larger, this component corresponds to 1% or less of the total signal intensity (see Figure 7), a number that cannot be identified with either of the two fractions of fluid, either extra- or intraparticle. It may possibly be related to a slowly exchanging reservoir in a region of low porosity and/or small pore size. Due to the difficulty in assigning this fraction, it is reasonable to state that diffusion exchange is almost completed after 50 ms (see Figure 7, more than 99% contribution of the dominating fraction), and that this averaged diffusion coefficient is slightly reduced due to tortuosity effects when the rms displacement exceed the distance between interparticle pores (typically on the order of the pore size, i.e. 20 nm).

Diffusion of *n*-Hexane in SiO_2/PSA Core-Shell Particles

The results of *n*-hexane diffusion in SiO_2/PSA core-shell system measured by the PFG NMR stimulated echo sequence for different diffusion times are shown in Figure 8.

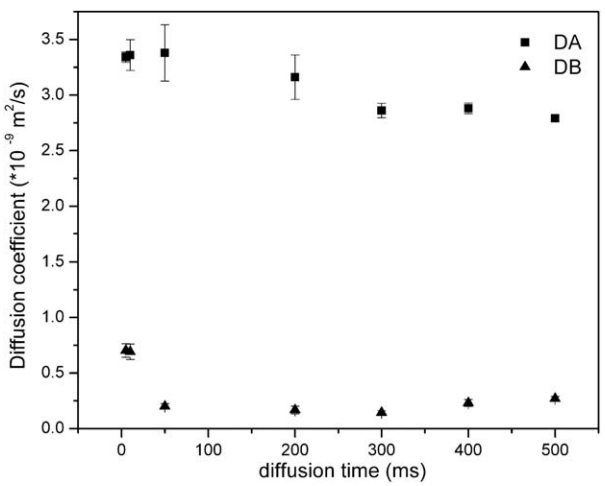

Figure 6. Diffusion coefficients as a function of diffusion time in SiO_2 system. The symbols are values extracted from biexponential fits of stimulated echo decays.

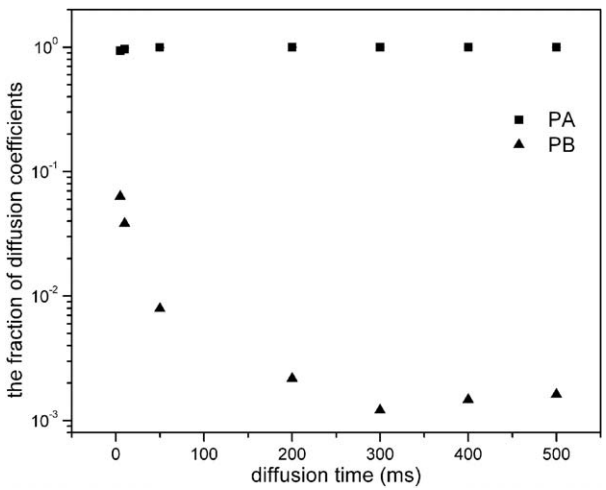

Figure 7. The fractions of diffusion coefficients at different diffusion times in SiO_2 system. The symbols are values extracted from biexponential fits of stimulated echo decays.

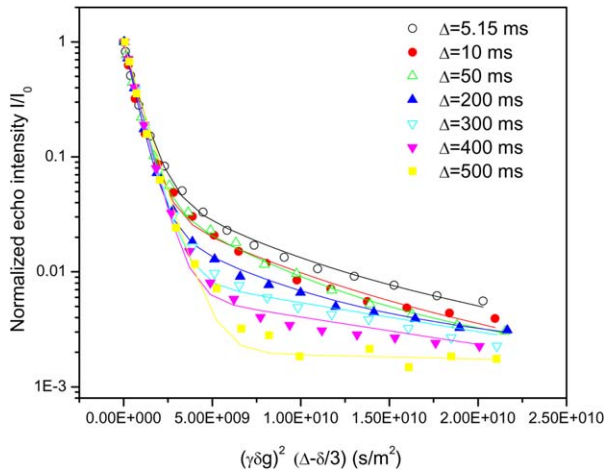

Figure 8. Echo decay curves of the PFG stimulated echo sequence in SiO_2/PSA system. The solid line is the result of biexponential fits to each decay curve. [Color figure can be viewed in the online issue, which is available at wileyonlinelibrary.com.]

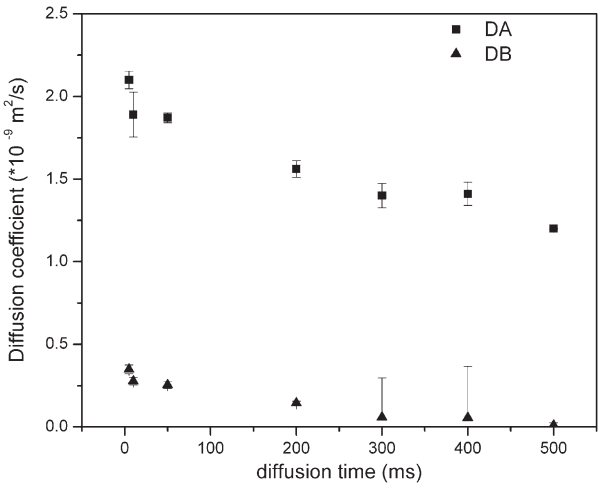

Figure 9. Diffusion coefficients as a function of diffusion time in SiO_2/PSA system. The symbols are values extracted from biexponential fits of stimulated echo decays.

As listed in Table III, the rms displacements obtained for the fitted values are in excess of 1 μm even for the shortest diffusion times. So that exchange from the 2 μm thick PSA coating layer is expected; the true value of the diffusion coefficient inside this layer is thus not accessible to the experiment, and is supposed to be smaller than the lowest fitting value. This argument is based on the assumption that molecular exchange through the coating interfaces is purely statistical. Due to exchange effects, the value of D_A is continuously decreasing for all diffusion times (see Figure 9). Its smaller initial value may be an indication for the reduced available interparticle space due to swelling of the PSA membrane. The subsequent decrease of D_A, on the other hand, hints at the exchange with the "slower" reservoir (SiO_2 and PSA membrane combined). The results show that, compared with the SiO_2 system, the presence of the PSA membrane acts both as a barrier that prolongs exchange (even at 500 ms, D_A is still changing), and as a volume that slows down diffusion in general. For long times, when all molecules have exchanged to show a single diffusion coefficient, this asymptotic value is expected to be considerably lower than in the system with uncoated SiO_2 particles which, at 500 ms, has practically reached this asymptotic value.

As shown in Figure 10, the fraction of D_B is rather small. This indicates that the amount of *n*-hexane molecules in the PSA membrane is very small. Low porosity of PSA is one reason for the small fraction. On the other hand, the averaged relaxation times of *n*-hexane obtained in this work (see above) indicate a T_2 of a few ms and a T_1 of 500 ms inside the PSA membrane. This short relaxation time, combined with a long "lifetime" (residence time) in the PSA membrane, leads to effective signal decay. As a result, the signal intensity from the *n*-hexane in the PSA membrane is reduced by a constant factor. Consistently, the fraction of D_B decreases with the longer observation time. Comparing Figures 7 and 10, the relative fractions approach a similar value but they decay much slower in Figure 10 because of the PSA acting as a barrier.

Interpretation of Diffusion Results of *n*-hexane in Silica and Core-Shell Particles

Although two diffusion coefficients are obtained both in SiO_2 and SiO_2/PSA systems, gradual exchange leads to averaging of these components. Averaging is almost complete for the longest diffusion time under consideration (500 ms) in the SiO_2 system, but not yet in the SiO_2/PSA system. A further gradual decay of the averaged quantity is expected until the rms displacement is much larger than the bead diameter; this situation is not reached in any of the investigated cases. This decay, however, has purely geometrical reasons and is strictly a function of the

Table III. The Calculated Diffusion Coefficients of *n*-Hexane in SiO_2/PSA System

Diffusion time (ms)	D_A ($\times 10^{-9}$ m^2/s)	rms Displacement (μm)	D_B ($\times 10^{-9}$ m^2/s)	rms Displacement (μm)
5.15	2.10	4.65	0.348	1.89
10	1.89	6.15	0.277	2.35
50	1.87	13.67	0.254	5.04
200	1.56	24.98	0.144	7.59
300	1.40	28.98	0.0582	5.91
400	1.41	33.58	0.0547[a]	6.62
500	1.20	34.64	0.00811[a]	2.85

[a] The results for 400 and 500 ms should be similar. This difference is included in the error bars, as shown in Figure 9.

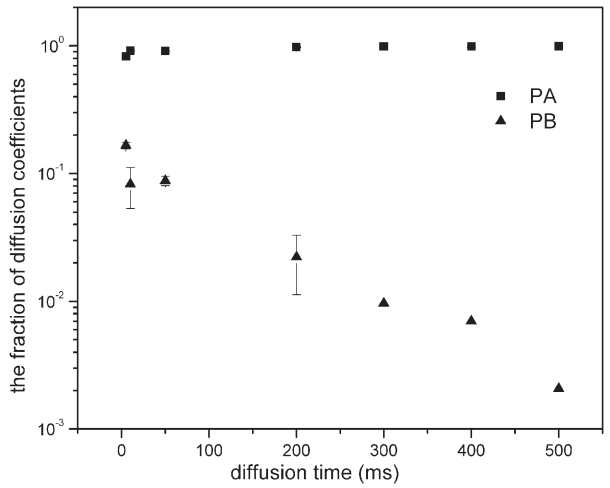

Figure 10. The fractions of diffusion coefficients at different diffusion times in SiO_2/PSA system. The symbols are values extracted from biexponential fits of single echo decays.

packing density of the system. Furthermore, a somewhat smaller intraparticle diffusion coefficient is found in the SiO_2/PSA system and can be attributed to the known swelling properties of PSA, where the coating is swelling and reducing the diffusion paths after addition of *n*-hexane; the shape of the pore space thus deviates from a random packing of hard spheres, and the overall free volume becomes smaller.

In the SiO_2/PSA system, a three-component ansatz should be made but even for the shortest diffusion times accessible in the experiment, partial exchange between the PSA membrane and its surroundings takes place. The estimated relaxation times in all three phases can potentially affect the correct derivation of relative weights of the individual diffusion components, but do not lead to a qualitative change of the observed behavior. The observed fitting data are understood as the result of partial mixing between phases A and C on the one hand, and A and B on the other hand. Full equilibration would require molecules to cross between the SiO_2 pore space and the interparticle space and vice versa, penetrating the PSA barrier layer with its smaller porosity and small pore size. Full exchange between the three phases is not achieved for the longest diffusion time and is thus expected to take significantly longer than 500 ms.

CONCLUSIONS

Polymer-coated SiO_2 particles with a core-shell structure were prepared based on phase inversion principles. Compared with the SiO_2 particles, the presence of PSA membrane reduced the BET surface area, the pore volume as well as the pore size distribution of polymer-coated SiO_2 particles from measurements of the nitrogen adsorption. Pulsed field gradient NMR was applied to detect the relaxation and diffusion of liquid in polymer-coated SiO_2 and SiO_2 particles under equilibrium conditions, in order to investigate the effect of polymer layer. The *n*-hexane molecules were used as probe molecules. The results of *n*-hexane relaxation experiments demonstrated that the presence of PSA sharply reduced the spin lattice relaxation time (T_1). The mobility of *n*-hexane molecules, especially the rotation of *n*-hexane, was limited by the PSA membrane. However, these changes were not sufficient to qualitatively affect the diffusion measurements that were carried out as a function of diffusion time between 5 and 500 ms. An analysis of the diffusion decays by biexponential fitting was attempted; the results were discussed in apparent diffusion coefficients and apparent relative weight fractions. The true values could not be obtained due to the fact that even at the shortest diffusion times, significant exchange between the different domains of the particles (21 μm diameter, 2 μm shell thickness) takes place. At 500 ms diffusion time, exchange is almost complete for the uncoated SiO_2 spheres, with the exception of a rather small amount ($<<1\%$) of *n*-hexane molecules with a much smaller diffusion coefficient present in a heterogeneous possibly weakly connected environment within the particles. For *n*-hexane in polymer-coated SiO_2 particles, the diffusion was much slower than in the SiO_2 particles. On one hand, the value of diffusion coefficient in intra-particles was a half of that in SiO_2 particles owing to the swelling and barrier effect of PSA. On the other hand, the diffusion of *n*-hexane in the core (SiO_2) was limited by the PSA membrane, and complete exchange did not yet take place within 500 ms.

In summary, in combination with the relaxation experiments, the diffusion results of PFG-NMR indicated that the PSA membrane on polymer-coated SiO_2 particles played as a transfer barrier for the *n*-hexane molecules. Variation of the thickness and properties of the PSA membrane will allow a better understanding of the polymerization of bimodal polyethylene as generated in a single process.

ACKNOWLEDGMENTS

The financial support provided by the Project of National Natural Science Foundation of China (211762078) and the Fundamental Research Funds for the Central Universities (2009QNA4028) are gratefully acknowledged. Project Based Personal Exchange Programme (PPP) (20083070) supported by China Scholarship Council and Deutscher Akademischer Austausch Dienst are also gratefully acknowledged.

REFERENCES

1. Arruebo, M.; Galan, M.; Navascues, N.; Tellez, C.; Marquina, C.; Ibarra, M. R.; Santamaria, J. *Chem. Mater.* **2006**, *18*, 1911.
2. Qiang, W.; Wang, Y.; He, P.; Xu, H.; Gu, H.; Shi, D. *Langmuir* **2008**, *24*, 606.
3. Hickey, J.; Burke, N.; Stover, H. *J. Membr. Sci.* **2011**, *369*, 68.
4. Breen, M. L.; Dinsmore, A. D.; Pink, R. H.; Qadri, S. B.; Ratna, B. R. *Langmuir* **2001**, *17*, 903.
5. Li, X. G.; Zhang, Y.; Meng, M.; Yang, G. H.; San, X. G.; Takahashi, M.; Tsubaki, N. *J. Membr. Sci.* **2010**, *347*, 220.
6. Teng, H.; Wang, J.; Chen, D. M.; Liu, P.; Wang, X. C. *J. Membr. Sci.* **2011**, *381*, 197.
7. Sun, L.; Hsu, C. C.; Bacon, D. W. *J. Polym. Sci. Part A: Polym. Chem.* **1994**, *32*, 2127.

8. Mteza, S. B.; Hsu, C. C.; Bacon, D. W. *J. Polym. Sci. Part A: Polym. Chem.* **1996**, *34*, 1693.
9. Kashiwa, N. *J. Polym. Sci. Part A: Polym. Chem.* **2004**, *42*, 1.
10. Bohm, L. L. *Angew. Chem. Int. Ed.* **2003**, *42*, 5010.
11. Liu, C. B.; Tang, T.; Huang, B. T. *J. Polym. Sci. Part A: Polym. Chem.* **2001**, *39*, 2085.
12. Du, L. J.; Li, W.; Fan, L. N.; Jiang, B. B.; Wang, J. D.; Yang, Y. R.; Liao, Z. W. *J. Appl. Polym. Sci.* **2010**, *118*, 1743.
13. Guo, Y.; Zhang, X. Q.; Dong, W. M. *J. Mol. Catal. A* **2005**, *237*, 45.
14. Kaur, S.; Singh, G.; Makwana, U. C.; Gupta, V. K. *Catal. Lett.* **2009**, *132*, 87.
15. Lijun, D.; Wei, Q.; Jingdai, W.; Yongrong, Y.; Wenqing, W.; Binbo, J. *Polym. Int.* **2011**, *60*, 584.
16. Kiparissides, C.; Dimos, V.; Boultouka, T.; Anastasiadis, A.; Chasiotis, A. *J. Appl. Polym. Sci.* **2003**, *87*, 953.
17. Macedonia, M. D.; Moore, D. D.; Maginn, E. J.; Olken, M. M. *Langmuir* **2000**, *16*, 3823.
18. Karaiskakis, G.; Gavril, D. *J. Chromatogr. A* **2004**, *1037*, 147.
19. Jobic, H.; Paoli, H.; Methivier, A.; Ehlers, G.; Karger, J.; Krause, C. *Micropor. Mesopor. Mater.* **2003**, *59*, 113.
20. Sorland, G. H.; Hafskjold, B.; Herstad, O. *J. Magn. Reson.* **1997**, *124*, 172.
21. Choudhury, R. P.; Schonhoff, M. *J. Chem. Phys.* **2007**, *127*, 234702.
22. Choudhury, R. P.; Galvosas, P.; Schonhoff, M. *J. Phys. Chem. B* **2008**, *112*, 13245.
23. Wassenius, H.; Nyden, M.; Vincent, B. *J. Colloid Interface Sci.* **2003**, *264*, 538.
24. Donahue, K. M.; Weisskoff, R. M.; Burstein, D. *J. Magn. Reson. Imaging* **1997**, *7*, 102.
25. Shriver, D. F.; Drezdzon, M. A. The Manipulation of Air-Sensitive Compounds; John Wiley & Sons, Inc.: New York, **1986**.
26. Kimmich, R. NMR: Tomography, Diffusometry, Relaxometry; Springer-Verlag: Berlin, **1997**.
27. Baldwin, A. J.; Christodoulou, J.; Barker, P. D.; Dobson, C. M.; Lippens, G. *J. Chem. Phys.* **2007**, *127*, 114505.
28. Stallmach, F.; Karger, J. *Adsorption* **1999**, *5*, 117.
29. Skirda, V.; Filippov, A.; Sagidullin, A.; Mutina, A.; Archipov, R.; Pimenov, G. Restricted diffusion and molecular exchange processes in porous media as studied by pulsed field gradient NMR. In: Conner, W. C.; Fraissard, J., Eds.; Fluid Transport in Nanoporous Materials; Springer: Dordrecht, **2006**; Vol. 219, p 255.
30. Song, Y. Q.; Cho, H.; Hopper, T.; Pomerantz, A. E.; Sun, P. Z. *J. Chem. Phys.* **2008**, *128*, 052212.
31. Ren, X. H.; Bertmer, M.; Stapf, S.; Demco, D. E.; Blumich, B.; Kern, C.; Jess, A. *Appl. Catal. A* **2002**, *228*, 39.
32. Strange, J. H.; Rahman, M.; Smith, E. G. *Phys. Rev. Lett.* **1993**, *71*, 3589.